I. Angulo et al., "A Measurement-Based Multipath Channel Model for Signal Propagation in Presence of Wind Farms in the UHF Band," in IEEE Transactions on Communications, vol. 61, no. 11, pp. 4788-4798, November 2013, doi: 10.1109/TCOMM.2013.101113.130144.

A Measurement-based Multipath Channel Model for Signal Propagation in Presence of Wind Farms in the UHF Band

Itziar Angulo, *Member, IEEE,* Jon Montalbán, *Graduate Student Member, IEEE,*
Josune Cañizo, *Graduate Student Member, IEEE,* Yiyan Wu, *Fellow Member, IEEE,*
David de la Vega, *Member, IEEE,* David Guerra, *Member, IEEE,* Pablo Angueira, *Senior Member, IEEE,*
and Amaia Arrinda, *Senior Member, IEEE*

***Abstract*—Scattering signals on wind turbines may lead to degradation problems on the communication systems provided in the UHF band, such as terrestrial television broadcasting, broadband wireless systems or public safety services. To date, despite the continuous requests from the International Telecommunication Union for studies on this field, no channel model has been developed to characterize signal propagation under these particular conditions. In response to this necessity, this paper presents a complete Tapped Delay Line (TDL) channel model to characterize multipath propagation in presence of a wind farm, including novel scattering modeling and Doppler spectra characterization. As proved later, this channel model, which is based on both theoretical development and empirical data obtained in the surroundings of a real wind farm, is adaptable to the particular features of any case under study: wind turbine dimensions, working frequency, and relative location of the wind farm, transmitter and receivers.**

***Index Terms*—Channel models, Doppler measurements, Multipath channel, TSR Channel Model, Wind farms.**

I. Introduction

INTERFERENCE effects of wind turbines on communication systems, such as analogue or digital television broadcasting, have been largely reported in the literature. These degradation effects are due to the signal from the transmitter impinging on the wind turbine structure and being scattered in all directions. Moreover, these scattering signals are dynamic in nature because of the rotation of the blades, leading to a time varying propagation channel even for fixed reception [1]-[4].

Up to now, there are no available channel models to characterize the particular propagation conditions encountered in presence of a wind farm in the UHF band, where terrestrial television broadcasting and other mobile communication services are provided. Regarding international regulations, the International Telecommunications Union proposes in Recommendation ITU-R BT.805 [5] and in Recommendation ITU-R BT.1893 [6] simplified methods to estimate the potential degradation due to a wind turbine on analogue and digital television, respectively. However, these suggested methods have two main disadvantages: they account for only one wind turbine, without considering the contributions of all the turbines that compose a wind farm; and they do not model the time varying nature of the scattering signals. Thus, they cannot be considered as complete channel models. In fact, the ITU maintains an open question where further studies about these aspects are requested [7].

In response to this necessity, in 2009 and 2010 the University of the Basque Country UPV/EHU carried out a measurement campaign in the surroundings of a wind farm in order to a) characterize signal scattering from wind turbines and b) evaluate the potential degradation of the DVB-T service due to the propagation conditions in presence of a wind farm. A description of the field trials and the methodology to analyze the scattering signals from wind turbines based on measured DVB-T data can be found in [8], whereas the reception thresholds of the DVB-T service in presence of a wind farm are analyzed in [4]. However, the main contribution of the research efforts that have been made since then is the adaptable channel model presented in this paper.

The two main issues that should be dealt with for the channel model under consideration are the scattering model to account for the relative power of the scattered signals, and the Doppler spectrum model to characterize signal variability due to blade rotation for the different working regimes of the wind turbine, i.e., different rotor orientations, rotation speed of the blades, etc. This work addresses both issues, providing significant results that are validated against empirical data from the extensive measurement campaign.

With respect to the first, the classical scattering models used in the UHF band were both theoretically and empirically evaluated in [9], concluding that they do not provide realistic estimations of scattered signals from modern wind turbines. Accordingly, the scattering pattern of a wind turbine was analyzed by means of physical optics-based simulations in [10], obtaining that the scattered signals of higher amplitude are due to the mast. The obtained conclusions justify the necessity of proposing the novel scattering model of Section V.

Manuscript received February 20, 2013; revised April 18, June 18 and September 22, 2013.

This work was supported in part by the European Union FP7 (grant agreement n°296164), by the Spanish Ministry of Economy and Competitiveness (project TEC2012-32370), and by the Basque Government (SAIOTEK program).

I. Angulo, J. Montalbán, J. Cañizo, D. de la Vega, D. Guerra, P. Angueira and A. Arrinda are with the Signal Processing and Radiocommunications research group (TSR) of the University of the Basque Country (UPV/EHU), 48013 Bilbao, Spain (phone: +34 946017382; fax: +34 946014259; e-mail: itziar.angulo@ehu.es).

Y. Wu is with the Communications Research Centre, Ottawa, Canada (e-mail: yiyan.wu@crc.ca)

Regarding the time variability of the channel model, although several research studies about the spectral characteristics of the signals scattered by wind turbines are found in the literature [11]-[12], these studies are focused on higher frequency bands and solely consider monostatic Doppler conditions. Hence, an analysis of the spectral characteristics of the signals scattered in bistatic conditions in the UHF band is needed. In this respect, a generic Doppler spectrum model that characterizes the specific variability of the scattering signals from wind turbines with rotating blades was developed by the authors in [13]. Nevertheless, this model needs to be adapted for the estimation of new working conditions, as explained in Section VI.

This document is organized as follows. Section II gives a brief description of the acquisition and processing of the empirical source data. Next, Section III introduces the basic concepts of the analyzed propagation channel and the Tapped Delay Line (TDL) scheme. Section IV presents the proposal of an adaptable channel model to characterize signal propagation in presence of wind farms in the UHF band. This channel model requires the development of a new scattering model, described in Section V, and the characterization of the time variability by means of representative Doppler spectra, included in Section VI. Section VII describes the step-by-step implementation of the channel model, whereas Section VIII is focused on the practical application of the novel channel model. Finally, the conclusions of the paper are gathered in Section IX.

II. Empirical Source Data

The field trials in which the following analysis is based were carried out in two stages during spring 2009 and spring 2010. Regular DVB-T (Digital Video Broadcasting – Terrestrial) transmissions in the UHF band were recorded in the surroundings of a wind farm installed close to two television transmitters [8].

Thanks to the pilot carriers included in the DVB-T signal, the Channel Impulse Response (CIR) that characterizes the propagation channel can be estimated [14]. Due to the constant delays of the multipath components at each fixed reception point, the signals scattered by the different wind turbines can be identified and obtained from the CIR. Accordingly, the time variability of the scattered signals as blades rotate can be analyzed by considering successive CIRs [4],[8].

Measurements were taken in 26 different reception locations around the wind farm. In order to account for different wind conditions, signal recordings were carried out in these reception locations through various days. From each recorded DVB-T signal, scattering signals corresponding to the wind turbines installed closest to the transmitters were detected and stored. In total, the empirical data base is formed by 328 signals scattered by the wind turbines as their blades rotate, each of these scattering signals lasting 10 seconds.

More detailed descriptions of the field trials and the methodology to obtain the components scattered by each wind turbine from the CIR of the DVB-T signal can be found in previous references from the authors [4],[8].

III. Basis of the Proposed Channel Model

A. Propagation Channel Characteristics

The propagation channel to be modeled corresponds to static reception in rural or semi urban environments in the surroundings of a wind farm. In presence of wind turbines, the propagation channel shows different characteristics whether the receiver is located in the forward scattering zone or in the backscattering zone [4],[15]. It has been proved that the propagation channel in the backscattering zone might be more demanding in terms of carrier-to-noise ratio (CNR) than the channel models proposed to test the DVB-T system. By contrast, the effects on quality degradation do not seem to be significant in the forward scattering area [4].

In the backscattering zone, the signals scattered on the wind turbines reach the receiver as attenuated, delayed and phase shifted replicas of the direct signal from the transmitter, i.e., a discrete multipath channel is encountered. For static reception in a certain location, the delays of the multipath components are constant. Nevertheless, the amplitude of each of these components depends on a set of fixed factors such as the relative position of the transmitter, the wind turbine and the receiver or the dimensions and materials of the wind turbine components; but also on a set of varying factors such as the orientation of the rotor with respect to the wind or its rotational speed. In fact, the rotation of the blades causes periodic variations in the amplitude and phase of the multipath components [8].

Therefore, it is necessary to propose a novel channel model to characterize signal propagation in the backscattering zone of wind turbines. Indeed, the typical channel models used to represent time-varying channels normally account for the mobility of the receiver [16]-[17], and thus do not apply to the particular features of signal propagation in presence of a wind farm. It should be noted that although the term backscattering is sometimes used to refer to monostatic situations, the term backscattering zone as used in this paper refers to bistatic conditions, and covers about 80 percent of the region around the wind turbine [15],[18].

B. Tapped Delay-Line Model

We are dealing with a multipath channel composed of a constant number of discrete resolvable components with constant delay and variable tap gains. The lowpass-equivalent impulse response of a discrete multipath channel composed of N components is given by [19]

$$\tilde{c}(t,\tau) = \sum_{k=1}^{N} \tilde{a}_k(t)\delta(\tau - \tau_k) \tag{1}$$

where, in our case, $\tilde{a}_k(t)$ represents the time-varying scattering signal from k-th wind turbine measured in the receiver position, and τ_k is the relative delay of this scattering signal, except for k=0, which corresponds to the direct signal from the transmitter.

The time-varying multipath channels can be described by TDL channel models. In a TDL model, a set of discrete paths is defined, each of which has a certain delay and

attenuation level. Furthermore, each path has an associated Doppler spectrum to account for the channel variability due to the movement of the transmitter, the receiver, or the environment [19]-[21]. Usually, TDL channel models provide just a set of fixed paths with representative delays, amplitudes and Doppler spectra for a general characterization of a certain reception environment [16]-[17]. Based on this generic TDL scheme, the main advantage of the channel model proposed in this paper is that it can be adapted to the particular features of any case under study.

IV. A Channel Model for Signal Propagation in Presence of Wind Farms

As previously mentioned, the proposed channel model is based on the TDL scheme, and it can be suited to a certain transmitter potentially affected by a wind farm and for each reception location within its coverage area according to the following parameters.

- *Number of paths*: The number of multipath components is found from the number of wind turbines whose backscattering zones include the reception location, plus the direct path corresponding to the signal from the transmitter.
- *Relative delays of the paths*: The relative delay of each multipath component is calculated as a function of the distance difference between the direct path (transmitter-receiver) and the path of the scattered signal (transmitter-wind turbine-receiver).
- *Mean amplitude of the paths*: The amplitude of each of the multipath components is the mean power of the scattering signal from the corresponding wind turbine measured in the receiver. The signal scattering on the wind turbine can be modeled by means of a scattering pattern which relates the incident signal on the turbine to the signal scattered in all directions.
- *Doppler Spectrum*: The Doppler spectrum represents the power spectral distribution of the scattered signals, and determines the temporal variability of the multipath components due to the rotation of the blades.

According to the previous approach, two main issues should be addressed: obtaining a scattering model that will truly characterize signal scattering from modern wind turbines, and finding a bistatic Doppler spectrum model to account for the movement of the blades and the nacelle for the different working regimes of the wind turbine.

V. Scattering Model

In the literature, several scattering models to account for the effect of a wind turbine on a signal transmitted in the UHF band are found: the scattering models included in the Rec. ITU-R BT.805 [5] and in the Rec. ITU-R BT.1893 [6], and the scattering models proposed by Van Kats [2], Sengupta [18], and the British Broadcasting Corporation (BBC) [22]. However, these scattering models suffer from several theoretical limitations. Furthermore, the empirical evaluation of these scattering models proves that they fail to provide accurate estimations of the signal scattered by modern wind turbines [9].

Moreover, in contrast to the assumptions of the above mentioned theoretical scattering models, accurate simulations of the scattering pattern of an actual wind turbine, based on physical optics theory, show that the metallic mast contribution is significantly higher than the contributions of its other components [10]. For this reason, the scattering model proposed in this paper is based on the signal scattered by the mast. This does not only reflect better the actual design and composition of modern wind turbines, but also allows considering the effect of the rotating blades separately, by means of the characterization of the Doppler spectrum of the scattering signals (as shown in Section VI).

A. Theoretical Basis of the Proposed Scattering Model

The signal scattered by the mast is represented by the Radar Cross Section (RCS) of a circular cylinder. The RCS is the projected area required to intercept and isotropically radiate the same power as a scatterer (target) scatters toward the receiver, and thus it is normally expressed in dB with respect to a square meter (dBsm) [23].

The formal definition of radar cross section states that the distance between the radar and the object must become infinite in order to eliminate any distance dependence in the RCS characteristics, i.e., far field condition in the context of signal scattering must be fulfilled [23]. The far field condition requires that the object is illuminated by a plane wave. The far field distance R_0 is normally expressed as a function of the lateral dimension of the object D and the wavelength λ [9], according to (2)

$$R_0 = \frac{2D^2}{\lambda} \tag{2}$$

For the case under study, where transmission frequency is 800 MHz and the mast length is 55 m, the far field distance is approximately 16 km. However, the cases of impact in the UHF band occur for quite shorter distances between transmitters and wind turbines [4]. Therefore, near field effects must be taken into account and included in the scattering model.

1) Bistatic RCS of a Circular Cylinder: The proposed model is based on the physical optics approximation. Considering the assumptions of this high frequency method, in [24] the RCS pattern of an elliptic cylinder is obtained as a function of its dimensions and the angular positions of the transmitter and receiver in both the vertical and the horizontal planes (θ_t, ϕ_t, and θ_r, ϕ_r respectively). However, this expression is of indeterminate form for some combinations of transmitter and receiver angular positions. The spherical coordinate system used to specify incident and observation (scattering) directions is shown in Fig. 1.

The expression proposed in [24] was adapted to a circular cylinder and simplified to avoid indeterminate forms, as included in Appendix A. The resulting expression for the calculation of the bistatic RCS of a circular cylinder is given by (3),

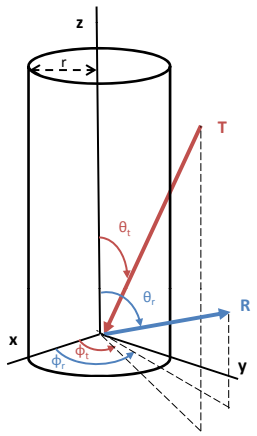

Fig. 1. Spherical coordinate system for the cylinder

$$\sigma(\phi_r,\theta_r,\theta_t) = 2krL^2\sqrt{\frac{1+\cos\phi_r}{2}}\cdot\frac{\sin^2\theta_t}{\sin\theta_t+\sin\theta_r} \cdot \operatorname{sinc}^2\left(\frac{kL(\cos\theta_t+\cos\theta_r)}{2}\right) \quad (3)$$

where $k = 2\pi/\lambda$, λ is the wavelength, r is the cylinder radius and L is the cylinder length.

According to the physical optics theory, the accuracy of RCS estimations err by wider margins as the direction of observation moves farther away from the specular direction [23]. In order to define the application limits of (3), the characteristics of the shapes corresponding to the horizontal and vertical planes of the cylinder have been considered. For the horizontal plane, the limit established for a sphere is used, in such a way that $-120° < \phi_r < 120°$ [25]. For the vertical plane, a flat plate can be taken as a reference, for which the physical optics theory performs quite well in predicting the returns in the region at within 20 or 30 degrees to either side of normal incidence, i.e., $70° < \theta_t < 110°$. Considering a similar margin for the bistatic case, the receiver angular position should be 20° to either side of the specular direction ($\theta_r = 180° - \theta_t$), in such a way that $160° - \theta_t < \theta_r < 200° - \theta_t$.

The graphic representation of the model proposed in (3) is given in Fig. 2 for the dimensions of the wind turbine under study [4],[8], where application limits are depicted in red. It can be observed that the RCS pattern in the horizontal plane is almost constant, whereas the scattering pattern in the vertical plane has a directive narrow lobe for the specular direction [10].

2) Near Field Effects: Near field effects in the context of signal scattering and for monostatic reception result in a RCS reduction [26] which can be equivalent to consider a *near field size* instead of the real size of the object [27]. This *near field size* L_{nf} is calculated according to (4), where R is the transmitter to the scattering object distance and λ is the wavelength,

$$L_{nf} = \sqrt{\frac{\lambda R}{2}} \quad (4)$$

TABLE I
TSR SCATTERING MODEL

Near field condition $R < \frac{2L^2}{\lambda}$, being R the transmitter to wind turbine distance and L the cylinder length
$\sigma(\phi_r,\phi_t)_{nf} = krL_{nf}^2\sqrt{\frac{1+\cos\phi_r}{2}}\sin\theta_t$ being $k = 2\pi/\lambda$, λ the transmission wavelength, r the cylinder radius ϕ_r the receiver angular position in the horizontal plane, θ_t the transmitter angular position in the vertical plane and $L_{nf} = \sqrt{\frac{\lambda R}{2}}$
Application limits
$70° < \theta_t < 100°$ $-120° < \phi_r < 120°$ $160° - \theta_t < \theta_r < 200° - \theta_t$

Nonetheless, under near field condition, some additional effects on the scattering pattern are observed: not only the above mentioned reduction in the amplitude of the main lobe of the object's pattern, but also the periodic nulls of the sinc squared pattern are smoothed away with decreasing distances, and the amplitudes of the sidelobes of the pattern increase [15],[28],[29].

Taking into account these effects, the scattering pattern of the cylinder in the vertical plane represented in Fig. 2 will lose the directivity typical of the sinc function. That is to say, in near field conditions, the RCS value corresponding to the specular direction can be used for wider angular positions in the vertical plane [15],[28],[29]. Therefore, the proposal for applying near field effects to our novel scattering model is to estimate the RCS value corresponding to the near field size L_{nf} in the specular direction in the vertical plane ($\theta_r = 180° - \theta_t$), and use it within the application limits established by the physical optics theory in this plane.

B. Proposed Scattering Model

The novel scattering model for a wind turbine that is proposed for its implementation in the proposed channel model is based on the scattering from the mast under near field condition. An accurate and easy-to-implement expression for the assessment of the mean values of the multipath components due to the scattering signals from wind turbines has been obtained. Table I shows the expressions of the proposed model – called TSR, which stands for "Signal Processing and Radiocommunications" Research Group in Spanish – to characterize signal scattering by a wind turbine in the UHF band.

C. Validation of the Proposed TSR Scattering Model

In order to check the validity of the proposed model, it is compared to the empirical data obtained from the measurement campaign. A similar study was carried out and reported in [9] for the pre-existing scattering models prior to the proposal of this new TSR scattering model.

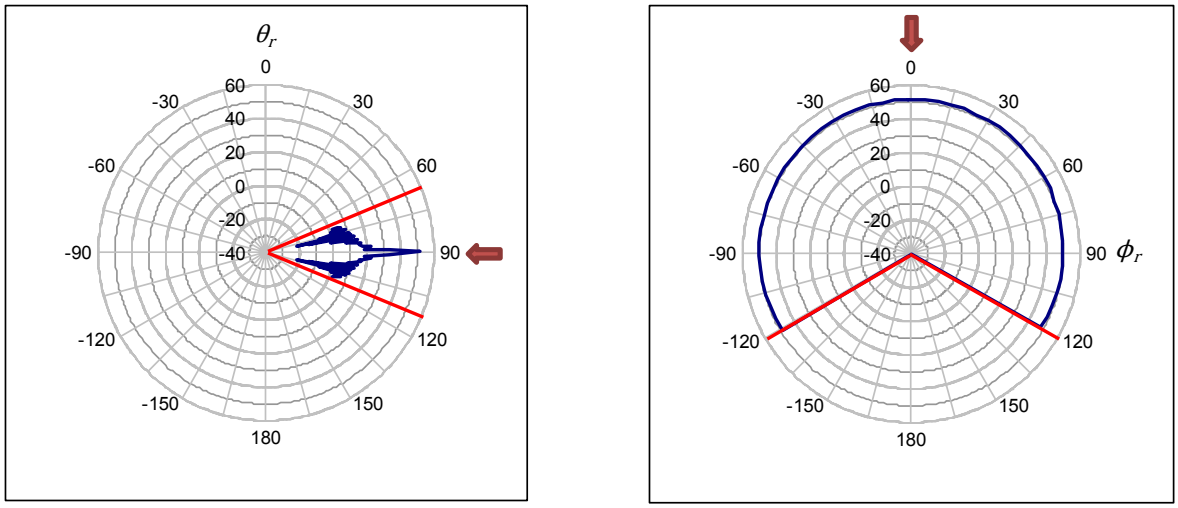

Fig. 2. Scattering pattern (RCS, dBsm) of the proposed expression for r=2.8 m, L=55 m and λ=0.38 m. Incident direction is represented by a red arrow. (left) vertical plane: RCS as a function of θ_r for $\phi_r = 0°$ (right) horizontal plane: RCS as a function of ϕ_r for $\theta_r = \theta_t = 90°$

TABLE II
STATISTICAL CHARACTERIZATION OF THE PREDICTION ERRORS OF THE SCATTERING MODELS

	Mean error	**Std. dev.**	**5^{th} / 95^{th} percentiles**	**% $\pm$6 dB**
Rec. ITU-R BT.805 [5]	6.4 dB	6.1 dB	-3.6 / 17.0 dB	45%
BBC [25]	14.5 dB	6.1 dB	5.9 / 24.7 dB	6%
Van Kats [2]	3.2 dB	6.1 dB	-5.5 / 13.3 dB	63%
Sengupta [15]	-5.2 dB	6.1 dB	-13.7 / 5.0 dB	49%
TSR	1.4 dB	5.8 dB	-6.5 / 11.4 dB	72%

The power of the signal scattered by a wind turbine is expressed as a carrier to interference ratio (C/I): the ratio in dB between the direct signal from the transmitter (the desired signal, referred to as carrier C) and the signal received after being scattered by the wind turbine (the interfering signal I) [9]. The results provided by all the scattering models are compared to the empirical values registered in the measurement campaign [8],[9]. Finally, a statistical analysis of the differences between the C/I_{pred} predicted by the theoretical models and the measured C/I_{meas} obtained by the estimation of the CIRs from the DVB-T signal is carried out.

The proposed TSR model has been developed in order to be independent of the variable conditions of blades rotation and different rotor orientations; all these variable conditions have been characterized by the Doppler Power Spectral Density of the scattered signal, analyzed in Section VI. Therefore, the validity of the scattering model will be assessed by evaluating the prediction error for each reception location, and then analyzing the global prediction error. For the statistical characterization of the prediction errors, the mean value, the standard deviation, the 5^{th} and 95^{th} percentiles and the percentage of errors between $\pm$6 dB are calculated. This statistical characterization of the prediction errors is shown in Table II.

From the results, it can be concluded that the TSR scattering model provides more accurate results than the pre-existing scattering models, with a mean error of approximately 1 dB. This is also noticeable when the $\pm$6 dB criterion is considered: 72% of the predicted values show absolute errors lower than 6 dB with respect to the empirical data. This result is almost 10% better than the next more accurate model proposed by Van Kats. It should also be noted that the standard deviation values are similar for all the analyzed models. This is probably due to the fact that the variability of the prediction errors is related to the inherent variability of the measurements and not to the scattering models [9].

Apart from providing more accurate results when compared to empirical data, it should also be highlighted that the TSR scattering model makes coherent assumptions with respect to the geometry and composition of the masts. The classical scattering models, by contrast, assume simplified geometries for the blades, representative materials and blades positions that do not reflect real conditions. Furthermore, in contrast to the computationally complex RCS estimation algorithms, the proposed TSR scattering model consists of a simple expression, which is suitable for its implementation in planning tools.

VI. DOPPLER SPECTRUM MODEL

The time variability of the channel is normally represented by Doppler spectrum models. In a previous reference from the authors, a generic Doppler spectrum model that characterizes the specific variability of the scattering signals from wind turbines with rotating blades was proposed and developed [13]. In this section, this novel spectrum model is briefly described, and the adaptation for its use in the proposed channel model is explained.

A. Characterization of Doppler Spectra of Scattering Signals from Wind Turbines with Rotating Blades

The novel spectrum model proposed in [13] is based on the empirical data obtained from the measurement campaign in the

surroundings of a wind farm, and applies to different working regimes and rotor orientations [8]. The estimated Doppler Power Spectral Densities (PSDs) correspond to near field condition with respect to transmitter-wind turbine distances, which differ from the spectral characteristics of the scattering signals in the far field [30]. However, as previously commented, it is precisely when near field conditions apply that more severe degradations on the telecommunication services may occur, and these conditions are of particular interest to the proposed channel model [4].

The common feature of all the estimated PSDs is the main component at 0 Hz, and lower power spectral densities for higher frequencies. The presence of this main component at 0 Hz, which is used for the normalization of the spectra, is due to the static part of the wind turbine, which validates our proposal of basing the scattering model on the mast [10]. The decreasing power levels for the higher frequencies are related to the movement of the blades, and are not necessarily symmetric with respect to 0 Hz due to their complex aerodynamic design [13].

In order to account for these special variability features of the scattering signals due to the rotating blades, a new exponential model was proposed in [13]. This model is composed of a Dirac delta for the zero Doppler frequency, and side components of decreasing power spectral density for the lowest and highest frequencies, according to (5)

$$S(f) = \begin{cases} a\exp(bf) - c, & f_{min} \leq f < 0 \\ \delta(f), & f = 0 \\ d\exp(-ef) - g, & 0 < f \leq f_{max} \end{cases} \quad (5)$$

where $S(f)$ is the PSD expressed in dB/Hz, a, b, c, d, e and g are positive constants, f stands for frequency (Hz), $\delta(0) = 0$ dB/Hz and f_{min} and f_{max} are the minimum and maximum observable Doppler shifts respectively. b and e represent the exponential decay (wider spectral characteristics for lower values and vice versa), c and g are related to the asymptotic values for infinite negative and positive frequencies, respectively, and a and d account for the relative value of the curve for the y-axis with respect to the asymptotic values for infinite frequencies given by c and g. The goodness of fit of this Doppler spectrum model has been validated by means of the estimation and characterization of an empirical data set of more than 300 complex scattered signals [13].

B. Minimum and Maximum Observable Doppler Shift due to Blade Rotation

For the model given by (5), the minimum and maximum observable Doppler shifts f_{min} and f_{max} were empirically obtained for each estimated PSD according to their spectral shape [13]. It should be taken into account that the theoretical bistatic Doppler shift f_B when the transmitter and receiver are stationary depends on the bistatic angular separation (transmitter-turbine-receiver), the rotor orientation with respect to this bistatic angular separation, the rotational velocity of the blades, the blades length, and the transmission wavelength. That is to say, the maximum Doppler shift varies from place to place for the same wind conditions, and also varies in a certain reception location for changing conditions of rotor orientation and/or rotational speed. Accordingly, a detailed calculation of the bistatic Doppler shift and consequently of the shape of the Doppler spectrum under the particular conditions of new situations and locations is not feasible.

However, for a given bistatic angular separation transmitter-wind turbine-receiver ϕ_r, the maximum bistatic Doppler shift f_{B_max} can be calculated as a function of the maximum rotation rate of the wind turbine ω_{max} and the blade length l, as given by (6)

$$f_{B\_max} = \frac{2\omega_{max} l}{\lambda} \cos(\phi_r/2) \quad (6)$$

Normalizing the estimated Doppler PSDs as a function of their corresponding maximum bistatic Doppler frequency shift f_{B_max} allows the estimation of new situations of time variability due to different working frequencies, wind turbine dimensions and relative locations transmitter-wind turbine-receiver. That is to say, in order to extend the applicability of the results, the maximum bistatic Doppler frequency shift f_{B_max} corresponding to the specific characteristics of a new case under study should be calculated according to (6), and the empirically estimated Doppler spectra adapted accordingly.

C. Doppler Spectra in the Proposed Channel Model

As previously commented, the Doppler spectrum of the signal scattered by a wind turbine depends on the relative location transmitter-wind turbine-receiver, the rotor orientation with respect to transmitter and receiver, and the blades rotational speed. Considering that both the rotor orientation and the blades rotational speed are dependent on the wind conditions, different levels of channel variability will be faced for a certain reception location in case of changing weather conditions. For this reason, the aim of this study is to provide the user of the channel model with a set of representative Doppler spectrum examples corresponding to the different levels of variability that will be faced in a fixed reception location.

The criterion used for the selection of representative cases is related to the impact of the time variability characterized by the different Doppler spectra on the potential degradation of the services provided in this frequency band. The potential degree of affection of the scattering signals on communication systems is directly connected to their level of variability. This degree of variability of the scattering signal is related to the spectral width of its Doppler spectrum, given by the difference between the minimum and the maximum observable frequency shifts f_{min} and f_{max}, and to the power spectral density values for the end frequencies [13].

Bearing this in mind, three representative PSDs were selected according to their spectral width and the relative power level for the end frequencies, and thus, to their potential degree of influence on the transmitted signals: low, medium or high. Taking into account that, for a given reception location, the most critical case would be encountered when the maximum observable Doppler frequency shift is f_{B_max}, the selected PSDs represent different levels of variability corresponding to approximately 90%, 65% and 30% of the maximum Doppler

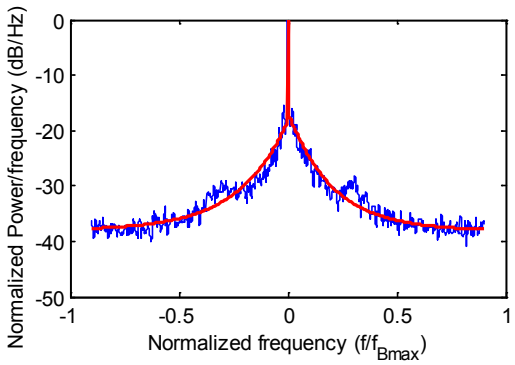

Fig. 3. Estimated PSD and exponential fitting corresponding to high variability conditions. $R^2 = 0.89$.

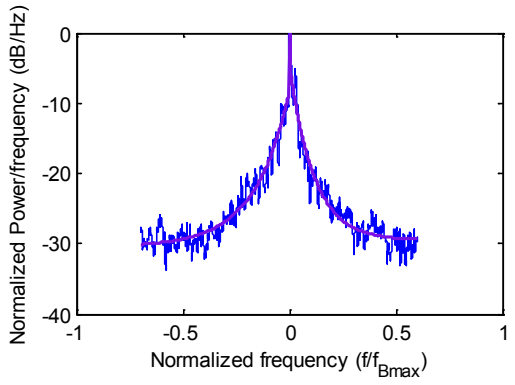

Fig. 4. Estimated PSD and exponential fitting corresponding to medium variability conditions. $R^2 = 0.93$.

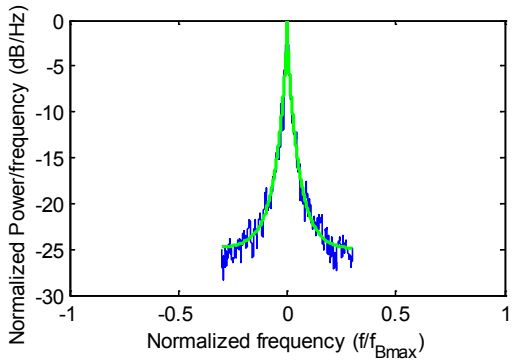

Fig. 5. Estimated PSD and exponential fitting corresponding to low variability conditions. $R^2 = 0.96$.

frequency shift. Figs. 3-5 show the estimated PSDs and the exponential fittings corresponding to high, medium and low variability, respectively. The normalized exponential fittings of the selected PSDs (expressed in dB/Hz) are shown in Table III.

VII. Implementation of the TSR Channel Model

In this section, the practical implementation of the TSR channel model for a certain case under study is described. More precisely, the methodology to obtain the parameters of the channel model for a certain reception location is detailed. This adaptation of the channel model to the particular characteristics of a case under study requires some input data, which is gathered in Table IV. Accordingly, the necessary parameters which are obtained from the input data of Table IV are included in Table V.

According to these data, the parameters of the channel model are adapted as following described:

TABLE III
Doppler PSDs Selected for the Channel Model

High variability

$$S_{high}(f) = \begin{cases} 19.7\exp(4.5\dfrac{f}{f_{B\_max}}) - 38.0, & -0.9f_{B\_max} \le f < 0 \\ \delta(f), & f = 0 \\ 21.4\exp(-4.8\dfrac{f}{f_{B\_max}}) - 38.1, & 0 < f \le 0.9f_{B\_max} \end{cases}$$

Medium variability

$$S_{med}(f) = \begin{cases} 22.0\exp(6.1\dfrac{f}{f_{B\_max}}) - 30.4, & -0.7f_{B\_max} \le f < 0 \\ \delta(f), & f = 0 \\ 25.1\exp(-8.7\dfrac{f}{f_{B\_max}}) - 29.5, & 0 < f \le 0.6f_{B\_max} \end{cases}$$

Low variability

$$S_{low}(f) = \begin{cases} 22.9\exp(17.9\dfrac{f}{f_{B\_max}}) - 24.9, & -0.3f_{B\_max} \le f < 0 \\ \delta(f), & f = 0 \\ 23.2\exp(-17.6\dfrac{f}{f_{B\_max}}) - 25.0, & 0 < f \le 0.3f_{B\_max} \end{cases}$$

A. Number of Paths

Regarding the number of paths, on a first approach, the total number of wind turbines of the wind farm should be considered. However, it should be checked that the reception location is in the backscattering zone of each wind turbine, dismissing the wind turbines out of the angular application limits of Table I.

B. Relative Delays of the Paths

The signal from the transmitter is taken as the reference for calculating the relative delays of each multipath component. Thus, for each wind turbine, the relative delay of the scattered signal is calculated as a function of the difference in distance between the direct path (transmitter-receiver) and the path of the scattered signal (transmitter-wind turbine-receiver) according to (7)

$$\tau_i = \frac{R_{Tx-WT_i} + R_{WT_i-Rx} - R_{Tx-Rx}}{c} \tag{7}$$

where τ_i is the relative delay of the signal scattered by i-th wind turbine, R stands for distances (see Table V) and c is the speed of light.

TABLE IV
INPUT DATA TO ADAPT THE CHANNEL MODEL TO THE SPECIFIC FEATURES OF A CASE UNDER STUDY

	Type	Description
For each wind turbine	Position	UTM (m) coordinates, including terrain height
	Mast dimensions	Vertical dimension of the mast (m)
		Lower and upper diameters of the mast (m)
	Blades length	Longitudinal dimension of the blades (m)
	Maximum rotation rate, ω_{max}	Maximum rotation rate of the blades (rpm)
Transmitter	Position	UTM (m) coordinates, including terrain height
	Radiating pattern	Radiating pattern of the radiating system of the transmitter
	Antenna height	Radiating system height within the telecommunication tower where it is allocated (m)
	Frequency, f	Working frequency within the UHF band (Hz)
	Power, P_t	Maximum transmitter power (W)
Receiver	Position	UTM (m) coordinates, including terrain height
	Radiating pattern	Radiating pattern of the radiating system of the receiver
	Antenna height	Radiating system height (m)

TABLE V
DATA CALCULATED FROM THE INPUT DATA OF TABLE IV

Symbol	Description
R_{Tx-WT_i}	For each wind turbine, transmitter to wind turbine distance (m)
R_{WT_i-Rx}	For each wind turbine, wind turbine to receiver distance (m)
R_{Tx-Rx}	Transmitter to receiver distance (m)
G_{Tx-WT_i}	Radiation pattern gain of the transmitter toward i-th wind turbine
G_{Rx-WT_i}	Radiation pattern gain of the receiver toward i-th wind turbine
G_{Tx-Rx}	Transmitter to receiver gain of the transmission radiation pattern
G_{Rx-Tx}	Maximum gain of the receiver radiation pattern
r	Mean radius of the mast
L	Length of the slanted surface of the mast, which is a truncated right circular cone
ϕ_r	Bistatic angle in the horizontal plane (transmitter-wind turbine-receiver), for each wind turbine
θ_t	Angular position of the transmitter in the vertical plane, with respect to each wind turbine
θ_r	Angular position of the receiver in the vertical plane, with respect to each wind turbine

C. Mean Amplitude of the Paths

The mean amplitude of the path corresponding to the direct signal from the transmitter is also taken as the power reference (0 dB). Hence, the mean amplitude of the remaining multipath components is given by the ratio, measured in the reception location and expressed in dB, between the power of the signal scattered from the corresponding wind turbine P_{Tx-WT_i-Rx} and the power of the direct signal from the transmitter P_{Tx-Rx}.

The direct power from the transmitter in the reception location, P_{Tx-Rx}, is calculated as a function of the transmitter to receiver distance R_{Tx-Rx}, the transmitter to receiver gain of the transmission radiation pattern G_{Tx-Rx}, the gain of the receiver radiation pattern G_{Rx-Tx} and the wavelength λ, including the corresponding additional propagation losses L_{prop} (such as diffraction losses due to terrain features), as shown in (8)

$$P_{Tx-Rx} = \frac{P_t G_{Tx-Rx} G_{Rx-Tx} \lambda^2 L_{prop}}{(4\pi)^2 R_{Tx-Rx}^2} \tag{8}$$

Then, for each wind turbine, the power of the scattered signal in the receiver location is calculated using the bistatic radar equation [15],[23],[28], according to (9)

$$P_{Tx-WT_i-Rx} = \frac{P_t G_{Tx-WT_i} G_{Rx-WT_i} \lambda^2 \sigma_i}{(4\pi)^3 R_{Tx-WT_i}^2 R_{WT_i-Rx}^2} \tag{9}$$

where P_t is the transmitted power, G stands for the different radiation pattern gains, R stands for distances (see Table V), and σ_i is the RCS of the mast in the receiver direction [10].

To calculate the RCS of the mast in the receiver direction, the incidence angle in the vertical plane (θ_t) as well as the reception angles in the horizontal and vertical planes (ϕ_r, θ_r) are calculated as a function of the position of the transmitter, the wind turbine and the receiver. The application limits of these angular positions and the near field condition should be checked (see Table I). For the transmission frequency and the corresponding distances and angular positions of the different elements, the bistatic radar cross section of that wind turbine for that reception location is obtained, as indicated in Table I.

Finally, the mean amplitude of each path P_i is given by the ratio of both powers: $Pi = P_{Tx-WT_i-Rx}/P_{Tx-Rx}$. Ratios lower than -45 dB can be neglected, as well as scattered power levels below the noise threshold.

D. Doppler Spectrum

For the characterization of the Doppler spectrum, representative PSDs corresponding to different levels of variability have been selected, as described in Section VI. These examples characterize increasing levels of variability due to different rotation rates and orientations of the wind turbine with respect to the transmitter and the receiver.

These Doppler spectra need to be suited to each reception location of new cases under study by calculating the corresponding maximum bistatic Doppler frequency f_{B_max}, which will depend on the relative position of the transmitter, the wind turbine and the receiver, the transmission wavelength, the maximum rotation rate, and the blade length (see (6) and Table V). This way, the Doppler spectra of Table III are to be adapted to the particular conditions of the new case under study by means of the specific value of f_{B_max}.

To account for the different wind conditions that will probably be faced for a certain reception location, it is recommended that the three PSDs provided in Table III are considered in the

channel model. In this way, the user of the channel model can obtain an overview of the different situations that may be encountered without the need for accurate estimations of wind directions or wind speeds.

VIII. Practical Application of the TSR Channel Model

As previously mentioned, the parameters of the TSR channel model have to be adapted to each reception location of the coverage area. To do so, a digital terrain database can be used to divide the coverage area of a potentially affected transmitter into small grids of a given accuracy. For each of the center locations of these grids, the parameters of the channel model for those specific conditions would be obtained, as explained in the previous section. This process is easily implementable in planning tools, and provides a fast overview of the potential degradation due to the wind farm.

Once the channel model has been adapted, the most complete way to estimate the impact on a certain service is to develop some simulations of the effect of the resulting time-varying channel model on the corresponding reception threshold. This implies obtaining a realization of the channel model, i.e., obtaining the successive channel impulse responses that characterize the signal propagation in presence of a wind farm. Getting back to Eq. (1) in Section III.B., the tap-gain processes $\tilde{a}_k(t)$ are obtained generating a set of white Gaussian processes, whose power spectral densities are shaped by a shaping filter whose amplitude transfer function is $H(f) = \sqrt{S(f)}$, where $S(f)$ is the Doppler power spectrum [19],[31],[32]. The resulting filter must have a normalized power of 1, so that the individual path gains have to be properly scaled to account for the different powers of the taps. Frequency-domain simulators use the Fast Fourier Transform (FFT) to perform convolution for the filtering operation of the generated complex Gaussian process [33].

A. DVB-T Case

One of the most important services provided in the UHF band is television broadcasting. Digital TV service coverage is characterized by a very rapid transition from near perfect reception to no reception at all, and it thus becomes much more critical to be able to define which areas are going to be covered and which are not [14].

For the specific case of DVB-T, the potential increment in the CNR threshold for Quasi Error Free (QEF) reception with respect to the typical Ricean channel used for the planning of fixed services [14] can be estimated as proposed in [4]. To do so, based on the estimated complex tap-gain processes obtained as mentioned above, the *multipath energy* and the *mean standard deviation* can be calculated as [4]:

$$P_{mult} = \sum_{i=1}^{N} P_i \tag{10}$$

where i=1 and $i = N$ are the indices of the first and last paths and P_i is the normalized mean amplitude from path i (in linear units), and

$$std_{mean} = \frac{\sum_{i=1}^{N} std_i}{N} \tag{11}$$

where i=1 and $i = N$ are the indices of the first and last paths and std_i is the standard deviation of the time varying complex tap gain from path i (in linear units)

Based on the obtained parameters, the maximum increment of the CNR thresholds over the theoretical Ricean CNR threshold can be predicted according to the results presented in [4]. Depending on the calculated *multipath energy* and *mean standard deviation* values, these increments can range from being negligible to being as high as 9 dB [4]. Therefore, this channel model provides a valuable tool to estimate the potential degradation on the DVB-T service, a potential degradation that is difficult to evaluate a priori due to the multiple factors that should be taken into account.

However, it should be remarked that although this study has been supported by measured DVB-T signals and this application case is also based on DVB-T, the proposed channel model is independent of the standard, and as such it is applicable to any service provided in the UHF band: terrestrial television broadcasting, broadband wireless systems or public safety services.

B. Common Application Scenarios

The application of this channel model is considered for two possible scenarios: planning of a new service on an area where a wind farm exists, or evaluation of the potential influence of a wind farm on a pre-existing service during the wind farm design process.

For the planning of a new service, according to the obtained results and depending on the quality target of that specific service, the required transmission power should be estimated. It should be also noted that increasing the transmitted power will not always mean to avoid the effect of the wind farm. Instead, it is necessary to diminish the power that reaches the wind turbines and increase the power transmitted towards the potential users of the service. In this respect, appropriate modifications in the radiation pattern of the transmitter may be more effective than an increase of the transmitted power.

In case of evaluation of the possible impact of a wind farm before its installation, if the quality is found to be potentially degraded, some preventive measurements can be taken, such as the relocation of some wind turbines, changes in the radiation pattern of the transmitter, etc.

IX. Conclusion

This paper proposes a channel model to characterize multipath propagation due to the presence of a wind farm in the UHF band, a study requested by the ITU since the first cases of impact [7]. To date, no channel model to describe signal propagation under these particular circumstances had been defined.

The most important feature of the TSR channel model is that it is adaptable to the particular features of any case under study, as the number of paths and their delays are calculated for

the specific features of the wind farm, the transmitter and the receiver sites. Moreover, the novel scattering model presented here provides the mean amplitude of the paths according to the specific features of the scenario, whereas the proposed Doppler spectra are also adjustable to the wind turbines' size, working frequency and relative positions of the transmitter, wind turbines and receivers.

This channel model has proved to be a valuable tool in order to estimate the potential degradation on a certain service due to the presence of a wind farm, a situation that is very difficult to evaluate a priori because of the multiple factors that are involved.

APPENDIX A

The RCS for an elliptic cylinder with semimajor axis a and semiminor axis b oriented with respect to the transmitter and the receiver as shown in Fig. 1 is given by (12) [24]

$$\sigma(\phi_t,\phi_r,\theta_t,\theta_r)=\frac{a^2b^2\lambda|e^{ikDL}-1|}{\pi D^2[(Aa)^2+(Bb)^2]^{\frac{3}{2}}}\{G_1^2+G_2^2+G_3^2\} \tag{12}$$

where $k=2\pi/\lambda$, λ is the transmission wavelength, L is the cylinder length and:

$$G_1=A(a_y\sin\theta_r\sin\phi_r+a_z\cos\theta_r)-B(a_x\sin\theta_r\sin\phi_r) \tag{13}$$

$$G_2=a_z\sin\theta_r(A\cos\phi_r+B\sin\phi_r) \tag{14}$$

$$G_3=B(a_x\sin\theta_r\cos\phi_r+a_z\cos\theta_r)-A(a_y\sin\theta_r\cos\phi_r) \tag{15}$$

$$A=\sin\theta_t\cos\phi_t+\sin\theta_r\cos\phi_r \tag{16}$$

$$B=\sin\theta_t\sin\phi_t+\sin\theta_r\sin\phi_r \tag{17}$$

$$D=\cos\theta_r+\cos\theta_t \tag{18}$$

For a circular cylinder, instead of semimajor and semiminor axes, it is only necessary to consider the cylinder radius r. Furthermore, the angular position of the transmitter in the horizontal plane can be taken as the reference, i.e. $\phi_t=0^\circ$, in such a way that the obtained expression is no longer dependent on ϕ_t. However, the resulting expression is still of indeterminate form for some combinations of transmitter and receiver angular positions.

As our main objective is to obtain a simple formula to be used for the channel model, we try to find separate expressions for the RCS patterns in the horizontal and vertical planes, to be later combined in a final expression.

If we consider that the incidence is orthogonal to the cylinder axis, i.e. $\theta_t=90^\circ$, the RCS pattern in the horizontal plane is given by (19)

$$\sigma(\phi_r)|_{\theta_t=\theta_r=90^\circ}=krL^2\sqrt{\frac{1+\cos\phi_r}{2}} \tag{19}$$

where $k=2\pi/\lambda$, λ is the transmission wavelength, r is the cylinder radius and L is the cylinder length.

Similarly, the RCS pattern in the vertical plane, assuming that both the transmitter and the receiver are located in the same vertical plane defined by $\phi_r=\phi_t=0^\circ$, is given by (20)

$$\sigma(\theta_r,\theta_t)|_{\phi_r=0^\circ}=2krL^2\frac{\sin^2\theta_t}{\sin\theta_t+\sin\theta_r}\cdot\operatorname{sinc}^2\left(\frac{kL(\cos\theta_t+\cos\theta_r)}{2}\right) \tag{20}$$

Combining (19) and (20) we obtain an approximate expression to characterize signal scattering in both the horizontal and vertical planes without indeterminate forms:

$$\sigma(\phi_r,\theta_r,\theta_t)=2krL^2\sqrt{\frac{1+\cos\phi_r}{2}}\frac{\sin^2\theta_t}{\sin\theta_t+\sin\theta_r}\cdot\operatorname{sinc}^2\left(\frac{kL(\cos\theta_t+\cos\theta_r)}{2}\right) \tag{21}$$

The simplified expression of (21) has been validated comparing it to the numerical evaluation of the bistatic RCS expression for an elliptical cylinder provided in [24]. This comparison has been made for the real dimensions of the wind turbines of the case under study [4],[8],[9], obtaining that the differences between both are less than 10% within the application limits of the proposed model, i.e., the differences are considered to be negligible.

ACKNOWLEDGMENT

The authors would like to thank the partners from Iberdrola Renovables for their continuous support and involvement in the study of the wind turbine effects on the radiocommunication services. Special thanks also to Itelazpi and Abertis Telecom for their kind collaboration in this work.

REFERENCES

[1] K. Cavcey, L. Y. Lee, and M. Reynolds, "Television interference due to electromagnetic scattering by the MOD-2 wind turbine generators," *IEEE Transactions on Power Apparatus and Systems*, vol. PAS-103, no. 2, pp. 407–412, 1984.

[2] P. Van Kats and O. Pager, "Reflections of electromagnetic waves by large wind turbines and their impact on UHF broadcast reception," *IEEE 1984*, pp. 91–99, 1984.

[3] M. Levent and I. Munro, "Effects of windmills on television reception," *CBC Technology Review*, vol. 1, pp. 1–8, Jan. 2006.

[4] I. Angulo, D. de la Vega, O. Grande, N. Cau, U. Gil, Y. Wu, D. Guerra, and P. Angueira, "Empirical evaluation of the impact of wind turbines on DVB-T reception quality," *IEEE Transactions on Broadcasting*, vol. 58, no. 1, pp. 1–9, 2012.

[5] International Telecommunication Union, "Assessment of impairment caused to television reception by a wind turbine," Rec. ITU-R BT.805, 1992.

[6] International Telecommunication Union, "Assessment of impairment caused to digital television reception by a wind turbine," Rec. ITU-R BT.1893, May 2011.

[7] International Telecommunication Union, "Conditions for a satisfactory television service in the presence of reflected signals," Question ITU-R 69-1/6, 2004.

[8] I. Angulo, D. de la Vega, O. Grande, Y. Wu, C. Fernandez, P. Angueira, and J. Ordiales, "Methodology for the empirical analysis of the scattering signals from a wind turbine," in *Antennas Propagation Conference, 2009. LAPC 2009. Loughborough*, 2009, pp. 553–556.

[9] I. Angulo, D. de la Vega, C. Fernandez, D. Guerra, Y. Wu, P. Angueira, and J. L. Ordiales, "An empirical comparative study of prediction methods for estimating multipath due to signal scattering from wind turbines on digital TV services," *IEEE Transactions on Broadcasting*, vol. 57, no. 2, pp. 195–203, Jun. 2011.

[10] I. Angulo, D. De la Vega, O. Rodriguez, O. Grande, D. Guerra, and P. Angueira, "Analysis of the mast contribution to the scattering pattern of wind turbines in the UHF band," in *Proceedings of the 5th European Conference on Antennas and Propagation (EUCAP)*, 2011, pp. 707–711.

[11] A. Naqvi, S.-T. Yang, and H. Ling, "Investigation of Doppler features from wind turbine scattering," *IEEE Antennas and Wireless Propagation Letters*, vol. 9, pp. 485–488, 2010.

[12] B. Gallardo-Hernando, F. Pérez-Martínez, and F. Aguado-Encabo, "Statistical characterization of wind turbine clutter in C-band radars," in *2008 International Conference on Radar*, 2008, pp. 360–364.

[13] I. Angulo, J. Montalbán, J. Cañizo, Y. Wu, D. de la Vega, D. Guerra, P. Angueira, and A. Arrinda, "Empirical Doppler characterization of signals scattered by wind turbines in the UHF band under near field condition,"*International Journal of Antennas and Propagation*, vol. 2013, Mar. 2013.

[14] ETSI, "Digital video broadcasting (DVB); framing structure, channel coding and modulation for digital terrestrial television," Tech. Rep. ETSI EN 300 744 V1.6.1, 2009.

[15] E. F. Knott, J. F. Shaeffer, and M. T. Tuley, *Radar cross section: its prediction, measurement, and reduction*. Norwood,MA: Artech House, Aug. 1985.

[16] M. Failli, *Cost 207 Digital Land Mobile Radio Communications: Final Report, 14 March 1984, 13 September 1988*. Office for Office Publ. of the European Communities, 1989.

[17] European Broadcasting Union, "Planning parameters for hand-held reception," Tech. Rep. EBU doc. Tech. 3317, Jul. 2007.

[18] D. Spera and D. Sengupta, "Equations for estimating the strength of TV signals scattered by wind turbines," Tech. Rep. NASA Contractor Report 194468, May 1994.

[19] M. C. Jeruchim, P. Balaban, and K. S. Shanmugan, *Simulation of Communication Systems: Modeling, Methodology and Techniques*. Springer, Oct. 2000.

[20] M. Pätzold, *Mobile Fading Channels*. J. Wiley, Apr. 2002.

[21] J. D. Parsons, *The mobile radio propagation channel*. Chichester; New York: J. Wiley, 2000.

[22] J. Eaton, R. Black, and G. Taylor, "Interference to television reception from large wind turbines," BBC Research Department, Eng. Division, Tech. Rep. BBC RD 1983/2, Mar. 1983.

[23] M. I. Skolnik, *Radar Handbook*. McGraw-Hill, Jan. 2008.

[24] K. M. Siegel, H. A. Alperin, R. R. Bonkowski, J. W. Crispin, A. L. Maffett, C. E. Schensted, and I. V. Schensted, "Bistatic radar cross sections of surfaces of revolution," *Journal of Applied Physics*, vol. 26, no. 3, p. 297, Mar. 1955.

[25] K. M. Siegel *et. al*, "Studies in radar cross sections VIII. theoretical cross section as a function of separation angle between transmitter and receiver at small wavelengths," Willow Run Research Center, University of Michigan, Tech. Rep. UMM-115, Oct. 1953.

[26] B. Welsh and J. Link, "Accuracy criteria for radar cross section measurements of targets consisting of multiple independent scatterers," *IEEE Transactions on Antennas and Propagation*, vol. 36, no. 11, pp. 1587–1593, 1988.

[27] E. Van Lil, D. Trappeniers, J. De Bleser, and A. Van de Capelle, "Computations of radar returns of wind turbines," in *3rd European Conference on Antennas and Propagation, 2009. EuCAP 2009*, 2009, pp. 3852–3856.

[28] E. F. Knott, *Radar Cross Section Measurements*. SciTech Publishing, 2006.

[29] P. Pouliguen, L. Lucas, F. Muller, S. Quete, and C. Terret, "Calculation and analysis of electromagnetic scattering by helicopter rotating blades," *IEEE Transactions on Antennas and Propagation*, vol. 50, no. 10, pp. 1396–1408, 2002.

[30] N. Whitelonis, S.-T. Yang, and H. Ling, "Application of near-field to far-field transformation to Doppler features from wind turbine scattering," *IEEE Transactions on Antennas and Propagation*, vol. 60, no. 3, pp. 1660 –1665, Mar. 2012.

[31] Y.-S. Choi, P. Voltz, and F. Cassara, "On channel estimation and detection for multicarrier signals in fast and selective rayleigh fading channels," *IEEE Transactions on Communications*, vol. 49, no. 8, pp. 1375–1387, 2001.

[32] G. Arredondo, W. Chriss, and E. Walker, "A multipath fading simulator for mobile radio," *IEEE Transactions on Communications*, vol. 21, no. 11, pp. 1325–1328, 1973.

[33] D. Young and N. Beaulieu, "The generation of correlated Rayleigh random variates by inverse discrete fourier transform," *IEEE Transactions on Communications*, vol. 48, no. 7, pp. 1114–1127, 2000.